Functional Imaging of Cancer with Emphasis on Molecular Techniques

Drew A. Torigian, Steve S. Huang, Mohamed Houseni and Abass Alavi

CA Cancer J Clin 2007;57;206-224
DOI: 10.3322/canjclin.57.4.206

CA: A Cancer Journal for Clinicians is published six times per year for the American Cancer Society by Lippincott Williams & Wilkins. A bimonthly publication, it has been published continuously since November 1950. *CA* is owned, published, and trademarked by the American Cancer Society, 250 Williams Street NW, Atlanta GA 30303. (©American Cancer Society, Inc.) All rights reserved. Print ISSN: 0007-9235. Online ISSN: 1542-4863.

Functional Imaging of Cancer with Emphasis on Molecular Techniques

Drew A. Torigian, MD, MA; Steve S. Huang, MD, PhD*; Mohamed Houseni, MD; Abass Alavi, MD*

Dr. Torigian is Assistant Professor of Radiology, Department of Radiology, University of Pennsylvania School of Medicine, Philadelphia, PA.

Dr. Huang is Nuclear Medicine Resident, Department of Radiology, University of Pennsylvania School of Medicine, Philadelphia, PA.

Dr. Houseni is Visiting Scholar in Nuclear Medicine, Department of Radiology, University of Pennsylvania School of Medicine, Philadelphia, PA.

Dr. Alavi is Professor of Radiology; and Director of Research Education, Department of Radiology, University of Pennsylvania School of Medicine, Philadelphia, PA.

This article is available online at http://CAonline.AmCancerSoc.org

ABSTRACT A multitude of noninvasive, quantitative, functional imaging techniques are currently in use to study tumor physiology, to probe tumor molecular processes, and to study tumor molecules and metabolites in vitro and in vivo using computed tomography (CT), magnetic resonance imaging (MRI), ultrasonography (US), positron emission tomography (PET), single-photon emission computed tomography (SPECT), and optical imaging (OI). Such techniques can be used in conjunction with structural imaging techniques to detect, diagnose, characterize, or monitor tumors before and after therapeutic intervention. These can also be used to study tumor gene expression, to track cells and therapeutic drugs, to optimize individualized treatment planning for patients with tumors, and to foster new oncologic drug development. In this article, we review the rich variety of functional imaging techniques that are available for these purposes, which are becoming increasingly important for optimal individualized patient treatment in this day and age of "personalized medicine." *(CA Cancer J Clin 2007;57:206–224.)*

To earn free CME credit for successfully completing the online quiz based on this article, go to http://CME.AmCancerSoc.org.

INTRODUCTION

Imaging technologies used to assess patients with cancer may be grossly subdivided into structural and functional imaging categories. Structural imaging entails the assessment of morphologic features of normal tissues and organs of the body and of malignant lesions within these structures. Computed tomography (CT), magnetic resonance imaging (MRI), and ultrasonography (US) are the prototypical imaging technologies that are currently used to perform oncological structural imaging. These can be used to assess the morphologic features of lesions and of changes in these features over time through use of serial imaging. However, structural imaging alone may not provide the clinician or researcher with all of the information that is necessary to fully characterize or monitor lesions in those with cancer or at risk for cancer.

As such, functional imaging has come into existence and is comprised of a multitude of noninvasive, quantitative imaging techniques that are currently in use to study tumor physiology, to probe tumor molecular processes, and to study tumor molecules and metabolites in vitro and in vivo. Functional imaging can be implemented through use of CT, MRI, and US, as well as through positron emission tomography (PET), single-photon emission computed tomography (SPECT), and optical imaging (OI). Such functional imaging techniques can be used in conjunction with structural imaging techniques, often in a synergistic fashion, to detect, diagnose, characterize, or monitor tumors before and after therapeutic intervention. These can also be used to study tumor gene expression, to track cells and therapeutic drugs, to optimize individualized treatment planning for patients with tumors, and to foster new oncologic drug development.

Disclosures: Dr. Huang was supported by a training grant through the National Institutes of Health (NIH) (T32-CA093258–03). Dr. Houseni was supported as a visiting scholar by the Ministry of Higher Education of Egypt.
*Please note that these authors have contributed equally to this manuscript.

In this article, we review the rationale for functional imaging of cancer, as well as the wide variety of functional imaging techniques that are available for use in the setting of cancer, which are becoming increasingly important for optimal individualized patient treatment in this day and age of "personalized medicine."

RATIONALE FOR FUNCTIONAL IMAGING OF CANCER

Cross-sectional structural imaging by CT, MRI, and US is currently used in standard clinical practice on a daily basis to qualitatively or semiquantitatively detect, characterize, stage, assess posttherapeutic response, and determine recurrence of malignant tumors based on structural features such as tumor shape, size, margins, location, spatial extent, attenuation (on CT), signal intensity (on MRI), echogenicity (on US), or gross degree of enhancement after intravenous administration of contrast agents. Despite its many contributions to the management of patients with cancer, structural imaging alone suffers from many shortcomings in such settings.

The first is that gross macroscopic changes in tissues or organs due to cancer generally lag in time following alterations at the molecular, subcellular, or cellular levels.[1,2] This has significant implications with regard to early detection of cancer for screening purposes, as well as for monitoring response to therapeutic intervention. The second is that macroscopic abnormalities are often nonspecific and often seen in nonneoplastic conditions. For example, enlarged lymph nodes in the setting of known malignancy may either be due to metastatic disease or benign hyperplasia.[3] The third is that data regarding physiology, biological processes, and molecular characteristics of tumors are not obtained. As such, structural imaging at a single time point may not provide adequate information regarding patient prognosis, probability of tumor response to therapeutic intervention, and new drug development. This shortcoming is exemplified by the Response Evaluation Criteria in Solid Tumors (RECIST) criteria to assess for tumor response to therapy based on unidimensional lesional size measurements. These criteria completely disregard functional imaging information about tumors that may be relevant to accurate definition of early tumor response.[4,5]

Fortunately, quantitative functional imaging techniques may be used with structural imaging techniques to maximize the amount and value of data acquired for tumor detection, characterization, staging, prognosis assessment, treatment planning, and early treatment monitoring, as well as for monitoring of cell trafficking (ie, how different types of cells distribute to various organ or tissue locations in the body) and new drug development. These techniques involve specialized applications of CT, MRI, and US, as well as SPECT, PET, and OI.

PET and SPECT are 2 types of emission computed tomography that are used to study the distribution of radiolabeled tracers within the body. PET radiotracers emit positrons that, after encountering electrons, lead to emission of 2 gamma rays directed at 180 degrees from each other. Sites of tracer accumulation in the body are thus determined by detection of these paired gamma rays, which is termed "coincidence detection." SPECT involves the use of radioisotopes that emit single gamma rays in arbitrary directions, thus requiring the presence of a metallic collimator to determine sites of tracer accumulation in the body. While the collimators provide directionality, they screen out most of the emitted photons. As a result of these features, SPECT generally has lower sensitivity than PET and is not as readily quantifiable as PET. Furthermore, in contrast to positron-emitting radionuclides, single photon-emitting radionuclides cannot be labeled to most biologically important compounds. This also limits its use both for clinical and research purposes.[2]

OI uses visible light to create images following administration of an agent that can be detected through fluorescence or luminescence. However, as biologic tissues are opaque to light at most wavelengths, only small animals that are relatively transparent to light, as well as structures superficially located in the human body within the lumina of hollow organs or along the external bodily surface, are generally amenable to OI.[6]

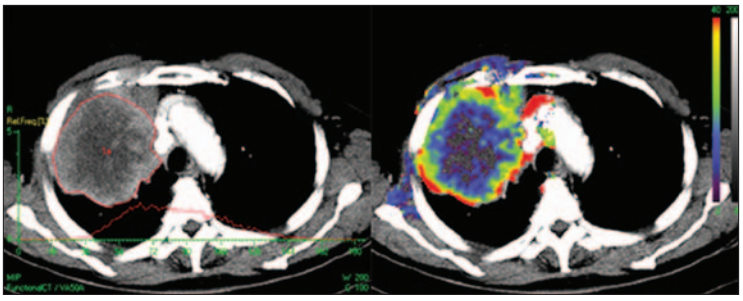

FIGURE 1 Computed Tomography (CT) Perfusion Assessment of Primary Lung Carcinoma. Left, axial CT image shows large, centrally necrotic lung carcinoma in right lung. Right, corresponding quantitative color parametric map overlaid on axial CT image shows varying permeability of lung carcinoma. Each pixel location within tumor corresponds to single quantitative perfusion value. Reproduced from Ng QS, Goh V, Fichte H, et al[17] with permission from the Radiological Society of North America.

FUNCTIONAL IMAGING TECHNIQUES TO STUDY TUMOR PHYSIOLOGY

Perfusion Imaging

Perfusion imaging may be used to improve detection and characterization of tumors, to monitor tumor response to therapeutic intervention, to improve delineation of residual or recurrent tumor, and to assess patient prognosis before and after treatment.[7,8] As such, MRI, CT, US, PET, SPECT, and OI have all been used to study the vascularity of malignancies. However, use of perfusion imaging techniques requires development of standardized measurement approaches in the context of prospectively specified, biologically valid endpoints.[9]

MRI has been commonly applied to study tumor perfusion through the dynamic contrast-enhanced MRI (DCE-MRI) technique, performed by acquiring images before, during, and after intravenous administration of a paramagnetic contrast agent (most often a gadolinium [Gd] chelate). This has been used to study various cancers where measurement of tumor microvascularity has been shown to correlate with tumor grade, microvessel density, tendency for metastasis and recurrence, levels of vascular endothelial growth factor (VEGF) expression, and survival outcomes.[10] For example, George et al reported that rectal tumors with higher permeability at presentation as measured on DCE-MRI appeared to respond better to chemoradiotherapy than those with lower permeability.[11] Perfusion MRI also has utility in the diagnosis and characterization of tumors. For instance, perfusion-weighted MRI has been used to differentiate pyogenic brain abscesses from cystic or necrotic brain tumors, which can be challenging when structural MRI features alone are used for this purpose.[12] Furthermore, effects of antiangiogenic and antivascular therapy can also be assessed with this technique.[9] As such, DCE-MRI has been used in clinical trials as an indicator of biological activity to assess the effectiveness of such therapies.[13]

Currently, CT is the most frequently used imaging tool for clinical assessment of the structural features of cancer. However, perfusion techniques can also readily be incorporated into existing CT protocols by acquiring images at multiple time points before and after intravenous administration of iodinated contrast agents.[14] Tumor angiogenesis correlates with tumor perfusion and vascular permeability, which can be assessed by determination of peak contrast enhancement and measurement of time-to-peak enhancement on dynamic contrast-enhanced CT (DCE-CT).[15] Measurements of tissue perfusion in tumors such as lung cancer have also been shown to correlate with markers of angiogenesis, such as VEGF expression.[16] Ng et al demonstrated that in non-small-cell lung carcinoma (NSCLC), quantitative whole-tumor assessment of vascular permeability and blood volume with CT is reproducible and may be useful to monitor effects of antivascular or antiangiogenic agents (Figure 1).[17] Perfusion CT analysis can also be applied to characterize lesions, and a primary example of this application is the assessment of the solitary pulmonary nodule. For example, Swensen et al reported that absence of significant enhancement (defined as ≤15 Hounsfield units) on CT at 1 to 4 minutes after contrast administration is strongly predictive of a benign histology.

US has been used to assess the velocity of flowing blood within vessels by measurement of the frequency (Doppler) shift of sound waves reflected from blood cells and can be applied to quantitatively study tumor vascularity.[18] In addition, quantitative estimation of tumor perfusion may be performed following the intravenous administration of sonographic contrast agents composed of encapsulated microbubbles that reflect sound waves.[19] For example, Su et al used

three-dimensional power Doppler US to monitor response of primary peritoneal papillary serous carcinoma to treatment and to differentiate residual tumor from post-treatment fibrosis.[20]

Perfusion imaging with SPECT and PET is performed with nontargeted tracers that have very high first-pass extraction, mostly for assessment of large organs such as the heart and brain where detailed spatial resolution is of limited value. With increasing availability of PET/CT and SPECT/CT instrumentation, perfusion and related imaging techniques can be carried out successfully in most clinical settings. However, the value of this approach in cancer diagnosis and management is presently unclear.

Diffusion Imaging

The random translational diffusion of water molecules can be quantitatively measured with diffusion-weighted MRI (DWI).[21] DWI provides indirect information about tissue structure, water content, and intra/extracellular space and can be used to estimate tumor cellularity and detect early changes following therapeutic intervention.[22] When cellular and subcellular compartmental membranes break down with necrosis or apoptosis, water molecules become less restricted to motion by diffusion.[21] However, when cellular swelling or an increase in tumor cellularity are encountered, water molecules become more restricted to motion by diffusion due to reduction in the extracellular space, where most of the translational movement of water molecules occurs (Figure 2).[23]

DWI was first used clinically to detect cellular changes due to acute cerebral infarction, but has also been applied to characterize tumors and monitor changes in tumors after therapeutic intervention, most often in the brain. For example, Hamstra et al performed DWI in patients with malignant glioma before and 3 weeks following the start of treatment with radiotherapy (often with chemotherapy, as well) and showed that changes in tumor diffusion at 3 weeks provided an early biomarker for tumor response, time to progression, and overall survival that correlated with structural imaging changes at 10 weeks.[24] DWI can also differentiate residual or recurrent brain tumor from treatment-induced damage to brain parenchyma following radiation therapy.[25] Furthermore, it has been used to differentiate pyogenic brain abscesses from cystic or necrotic brain tumors and to differentiate lymphomas from gliomas, as the former have more limited water diffusion due to a higher nuclear-cytoplasmic ratio.[26,27]

Through diffusion tensor MRI (DTI), anisotropic diffusion of water molecules in tissues such as the cerebral white matter (due to organization of myelinated axons in bundles) can be quantitatively measured, providing exquisite detail of tissue microstructure.[28] This is particularly useful for pretreatment planning for brain tumors through differentiation of peritumoral edema from infiltrative tumor, pretreatment assessment of white-matter tract involvement by tumor, and intraoperative visualization and localization of major white-matter tracts to decrease the chance of injury to normal tissues (Figure 2).[29]

DWI and DTI have been more difficult to use outside of the brain, in part due to increased motion artifacts.[28] For example, investigators have shown that DWI may provide information regarding extent of breast cancer, as well as early response to therapeutic intervention.[30,31] However, these applications are still under active investigation.

Functional Lymph Node Imaging

Lymph node imaging is of great importance for the staging of malignant tumors. However, assessment of lymph nodes based on structural imaging features alone is limited in sensitivity and specificity for microscopic metastatic disease. Hence, functional imaging techniques are currently under development to overcome these limitations.

Functional lymph node imaging has largely been performed with radiolabeled particles to identify nodes that most likely represent probable sites of metastasis. The best known is ^{99m}Tc sulfur colloid, which is used for conventional sentinel node imaging.[32] In the early stages of metastasis when the flow of lymph through an affected lymph node has not yet been altered, conventional sentinel node imaging can correctly identify this lymph node. However, as the number of cells in an affected lymph node

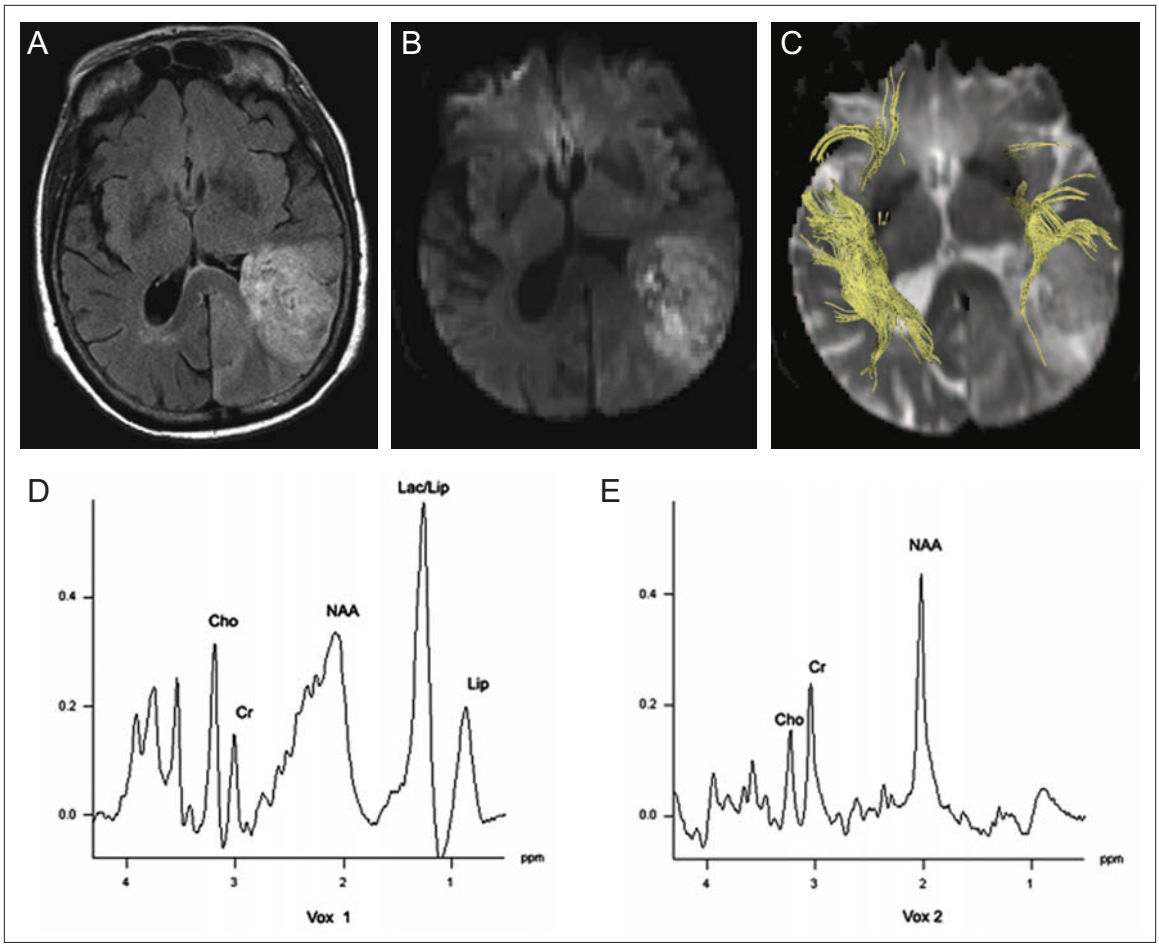

FIGURE **2** Magnetic Resonance Imaging (MRI) of Glioblastoma Multiforme Infiltrating and Displacing Left Superior Longitudinal Fasciculus (SLF) of Brain. (A) Axial fluid-attenuated inversion recovery image shows heterogeneous mass with surrounding edema. (B) Axial diffusion-weighted image demonstrates high signal intensity-restricted diffusion in tumor. (C) Fiber-tracking images show diminished SLF on left due to displacement and infiltration by tumor. (D) Representative MR spectrum from tumor voxel (vox 1) shows typical high-grade glioma spectral features of reduced N-acetyl aspartate (NAA, 2.0 ppm), increased choline (Cho, 3.2 ppm), increased lactate (Lac, 1.3 ppm), and increased lipid (Lip, 1.3 and 0.9 ppm) peaks. (E) Representative MR spectrum from voxel (vox 2) on contralateral normal side. Figures courtesy of Sumei Wang, MD, Gul Moonis, MD, and Elias R. Melhem, MD, PhD, University of Pennsylvania.

increases due to tumor growth, the flow of lymph through the node may be diverted to the next draining lymph node due to increased resistance, leading to lack of depiction of the originally involved sentinel lymph node. At this stage, blood supply to the involved lymph node is primarily provided by capsular arterial vessels to sustain the viability of cancer cells. Therefore, systemically administered compounds such as ^{18}F-2-fluoro-2-deoxy-D-glucose (FDG) will be directly delivered to these cancer cells and permit visualization of these sites of nodal involvement in the whole body. Thus, in such settings, conventional sentinel lymph node imaging is complementary with whole-body FDG-PET nodal imaging.[33]

However, these observations are based on preliminary results from a limited number of patients and thus will require further validation for clinical utility in the future.

A new agent to evaluate lymphatic drainage using MRI is ferumoxtran-10, a particular ultrasmall superparamagnetic iron oxide-based biodegradable nanoparticle composed of an iron oxide core and a dextran coating, which is an example of a nontargeted contrast agent that leaks into the interstitium and reaches the reticuloendothelial cells of lymph nodes via the lymphatic system, allowing for detection of micrometastases within normal-sized lymph nodes. Normal lymph nodes become dark in

signal intensity after ferumoxtran-10 administration due to shortening of T2 and T2* relaxation times of water protons, whereas metastatic deposits within lymph nodes remain bright.[34,35] This agent has been used to evaluate lymph nodes in the setting of a wide variety of malignancies. For example, Deserno et al showed that ferumoxtran-10-enhanced MRI significantly improved nodal staging in those with bladder carcinoma by depicting metastases even in normal-sized lymph nodes, with accuracy, sensitivity, specificity, and positive and negative predictive values of 95%, 96%, 95%, 89%, and 98%, respectively.[36] Also, Harisinghani et al reported that MRI with lymphotropic superparamagnetic nanoparticles correctly identified all patients with nodal metastases due to prostate carcinoma and that nodal analysis had a significantly higher sensitivity (90.5%) compared with conventional MRI (35.4%) (Figure 3).[34] Will et al performed a meta-analysis of prospective studies that compared MRI, with and without ferumoxtran-10, with histological diagnosis after surgery and biopsy and showed that ferumoxtran-10-enhanced MRI is sensitive and specific in detection of nodal metastases for a variety of tumors and offers higher diagnostic precision than unenhanced MRI for detection of lymph node metastases.[37] As such, ferumoxtran-10-enhanced MRI, like PET, has the potential to become a useful clinical functional imaging tool to evaluate lymph nodes of the whole body in the setting of cancer.

Conventional sentinel lymph node imaging will continue to be a very important technique to identify potential sites of regional nodal metastasis for malignancies such as breast cancer and melanoma. This technique, however, does not allow for direct detection of involved lymph nodes, but directs surgical exploration to nodal sites that are potentially most vulnerable to cancer spread. In contrast, FDG-PET or ferumoxtran-10-enhanced MR-based lymph node imaging allows for visualization of sites of nodal abnormality throughout the body. Whereas FDG-PET directly targets cancer cells in involved lymph nodes, ferumoxtran-10-enhanced MRI indirectly reveals cancer sites in lymph nodes. Therefore, the specificity of the latter may prove suboptimal in lymph nodes that are involved by nonneoplastic processes. As such, multicenter clinical trials are currently either in development or in progress as part of the ongoing safety and diagnostic performance assessment of the latter approach in relation to different types and locations of cancer.

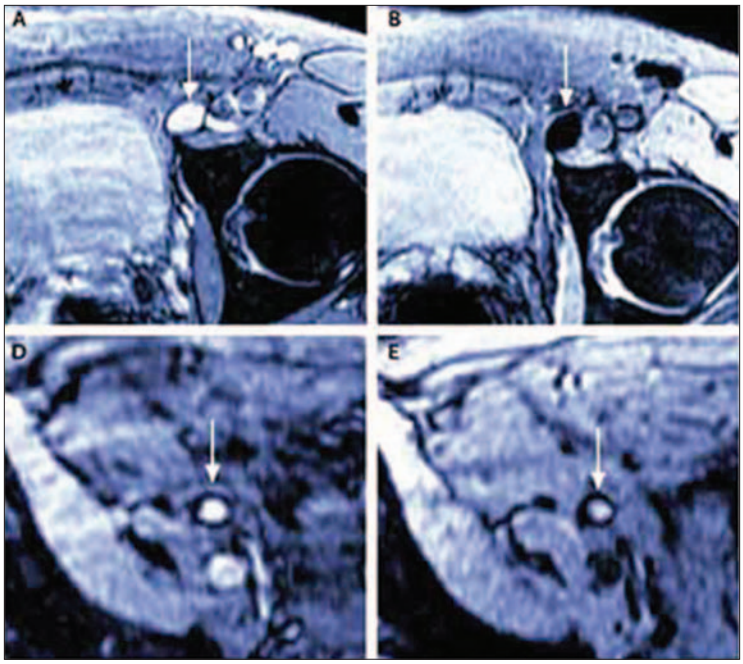

FIGURE 3 Magnetic Resonance Imaging (MRI) of Lymph Nodes in Two Different Patients with Prostate Cancer. As compared with conventional MRI (A), T2*-weighted gradient-echo MRI obtained 24 hours after administration of lymphotropic superparamagnetic nanoparticles (B) shows homogeneous decrease in signal intensity due to accumulation of lymphotropic superparamagnetic nanoparticles in normal lymph node in left iliac region (arrow). Conventional MRI shows high signal intensity in nonenlarged iliac lymph node completely replaced by tumor (arrow in D). Nodal signal intensity remains high (arrow in E) on T2*-weighted gradient-echo MRI following nanoparticle administration. Reproduced and modified from Harisinghani MG, Barentsz J, Hahn PF, et al[34] with permission from the *New England Journal of Medicine*.

FUNCTIONAL IMAGING TECHNIQUES TO PROBE TUMOR MOLECULAR PROCESSES

Metabolic Imaging

Metabolic imaging relies on differential utilization of various substrates through different biochemical pathways in cancer cells compared with normal tissue. In general, any small molecule that contains a radioisotope can be identified by various detection methods as it passes through biochemical pathways. Positron-emitting compounds dominate this category of tracer molecules, largely due to the feasibility of utilizing positron-emitting isotopes

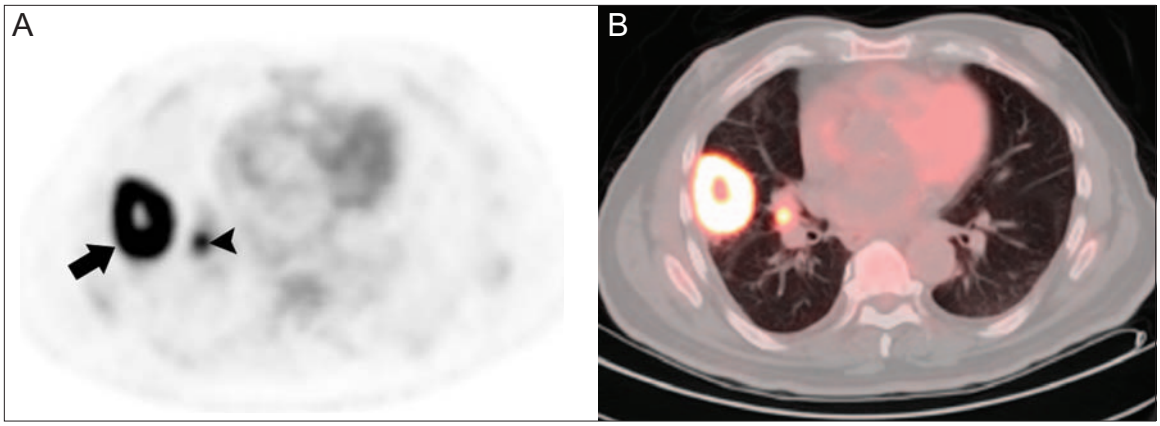

FIGURE **4** FDG-PET/CT Staging of Lung Carcinoma. (A) and (B) Axial FDG-PET and fused PET/CT images of patient with lung cancer show increased FDG uptake in 4 x 5 cm right lung cancer (arrow) with central necrosis. Note metabolically active right hilar lymph node (arrowhead), as well. Bilateral adrenal gland metastases also demonstrated FDG uptake (not shown).

such as ^{11}C and ^{18}F to replace nonradioactive carbon and hydrogen atoms, respectively, in any organic molecule. These positron-emitting analogues of metabolically relevant molecules can then be detected with PET in picomolar to nanomolar concentrations in vivo.[38] The superb sensitivity of this approach allows for administration of these positron-emitting compounds in nonpharmacologic concentrations and imaging of metabolic pathways without perturbation of cellular, subcellular, or molecular processes. A wide variety of metabolic tracers have been developed to target the transport and metabolism of glucose and amino acids.

Glucose Metabolism

FDG, a glucose analogue first tested in humans in 1976, is by far the most widely used metabolic tracer in the world.[39] Pioneering work since its conception has helped to solidify FDG-PET as a powerful diagnostic imaging modality in oncology and has sparked a growing interest in molecular imaging.[2] FDG-PET can be used to assess any malignancy that has accelerated glucose metabolism.

FDG is transported into cells via glucose transporters such as GLUT-1 and subsequently phosphorylated by hexokinase.[40] The metabolic product 2-fluorodeoxyglucose-6-phosphate is effectively trapped intracellularly, as it cannot undergo further metabolism through the glycolytic pathway. Persistent glucose uptake in many cancer cells in a low serum insulin state makes FDG an ideal tracer for cancer imaging. In fact, the Centers for Medicare and Medicaid Services (CMS) has approved reimbursements for diagnosis, staging, and restaging of lung cancer, esophageal cancer, colorectal cancer, melanoma, lymphoma, head and neck cancer, and breast cancer. Characterization of the solitary pulmonary nodule, restaging of noniodine-avid thyroid cancer, and evaluation of metastases in cervical cancer before therapy are also reimbursable by Medicare. Recently, the CMS has approved reimbursement for virtually all cancers if conducted in centers participating in certain patient registries such as the National Oncologic PET Registry (NOPR).

FDG-PET provides complementary information to structural imaging techniques for diagnosis and staging of cancer (Figures 4 and 5). For example, meta-analysis by Gould et al reported a sensitivity of 97% and a specificity of 78% for the evaluation of solitary pulmonary nodules.[41] In addition, meta-analysis by Toloza et al indicates that FDG-PET has an 84% sensitivity and an 89% specificity for mediastinal staging of NSCLC, whereas CT alone has a sensitivity and specificity of 57% and 82%, respectively.[42] The difference in sensitivities between metabolic imaging with FDG-PET and anatomic imaging using CT-size criteria highlights a typical advantage of metabolic imaging when compared with structural imaging. With its high sensitivity for metabolically active lesions, FDG-PET has also been shown to detect unexpected

extrathoracic metastases in 10% to 20% of patients and leads to changes in therapeutic management in about 20% of patients with lung cancer. In general, FDG-PET adds value to the staging workup of patients with relatively aggressive and metabolically active cancers such as lymphoma, melanoma, and breast, lung, head and neck, cervical, esophageal, or colorectal cancer by increasing the sensitivity for nodal and distant metastatic disease and by increasing the specificity for malignancy relative to the diagnostic performance of structural imaging alone. However, FDG-PET in general has lower sensitivity for slower growing, less metabolically active tumors such as prostate cancer, thyroid cancer, neuroendocrine tumors, and bronchioloalveolar cell lung carcinoma. FDG-PET is also particularly useful for restaging of malignancy because structural changes caused by surgery or radiation therapy may render anatomic imaging techniques inconclusive at most anatomic sites. Cancer restaging with FDG-PET has a general sensitivity of 80% to 95%, a specificity of 75% to 90%, and an accuracy of 80% to 90% for the detection of persistent or recurrent disease.[43] With the introduction of a recent generation of PET and PET/CT scanners, as well as well-established diagnostic criteria for interpretation of FDG-PET scans, the value of FDG-PET in evaluation of patients with cancer has been enhanced even more. Please note that a detailed review of the specific clinical indications for PET is beyond the scope of this article.

FDG-PET also provides complementary information to structural imaging techniques for cancer treatment planning. For example, FDG-PET in conjunction with CT or MRI is increasingly being used to define tumor volumes for radiation treatment planning. FDG-PET improves target-volume coverage at both the primary tumor level and regional lymph node level and tends to enlarge the radiation field when hypermetabolic normal-sized regional lymph nodes are identified. In fact, incorporation of both FDG-PET and CT images in target-volume selection has been shown to change treatment planning in over 50% of patients with Stage I to III NSCLC compared with treatment planning using CT alone.[44,45] FDG-PET can also lead to a reduction in radiation volume for primary tumors, with sparing of nonmalignant tissues. This is particularly true in the setting of lung tumors due to the ability to separate collapsed, fibrotic, or necrotic tissues from tumor, which may otherwise be indistinguishable using structural imaging alone (Figure 6).[46] Ciernik et al reported that in patients with head and neck cancer who were undergoing radiation treatment planning with CT, gross target volume (GTV) changed in 32% with addition of PET data, and the mean change in planning target volume (PTV) was 20%. Moreover, the interobserver variability in target-volume definition also improved when PET data were included.[45]

FIGURE **5** FDG-PET Staging of Non-Hodgkin Lymphoma. Coronal whole-body FDG-PET image shows multiple foci of increased FDG activity that correspond to lymph nodes throughout neck, axillae, mediastinum, retroperitoneum, and inguinal regions. Also noted are increased foci of FDG uptake in thoracic and lower lumbar spine in keeping with bone marrow metastases.

Degrees of FDG uptake in malignant lesions at baseline and during follow up after therapy may also be used to provide prognostic value. For example, in surveying 155 patients with NSCLC, Ahuja et al found that patients with standardized uptake values (SUVs) of less than

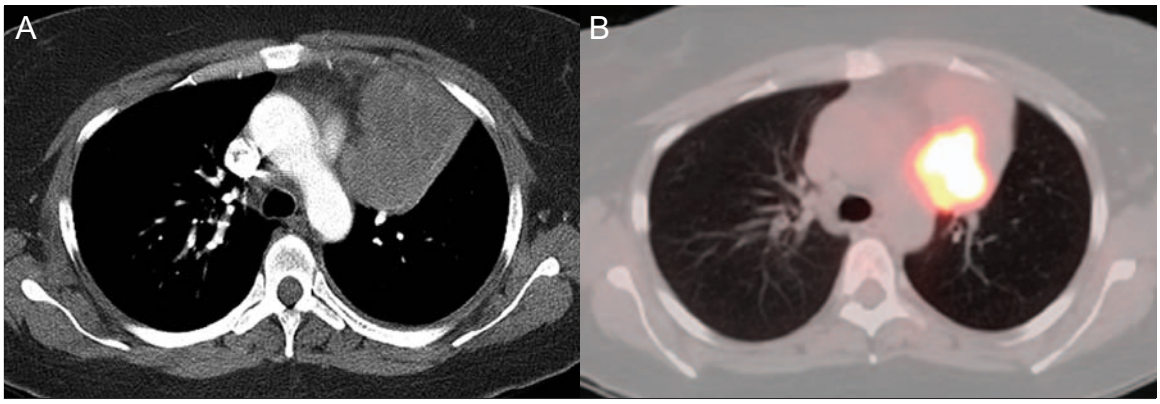

FIGURE **6** FDG-PET/CT of Lung Carcinoma for Radiation Treatment Planning. (A) and (B) Axial contrast-enhanced computed tomography (CT) image and corresponding fused PET/CT image allow one to differentiate completely atelectatic lung of left upper lobe and lingula from metabolically active central tumor. Whereas tumor is visualized with intense FDG uptake, atelectatic lung shows minimal metabolic activity.

10 in the primary lesion had a median survival of 24.6 months, whereas those with SUVs of more than 10 had a median survival of 11.4 months.[47] Although evidence suggests that FDG uptake from a single FDG-PET scan has prognostic value, threshold SUVs vary considerably in reported studies, limiting its clinical applicability. However, serial imaging, especially before and after treatment, is useful as a prognostic indicator in patients with cancer and as a means of monitoring therapeutic response (Figure 7).[48] Ceresoli et al noted that after 2 cycles of chemotherapy for mesothelioma, patients who had a metabolic response on FDG-PET had a median time-to-tumor progression of 14 months compared with 7 months for those without metabolic response.[49] Serial FDG-PET treatment monitoring has also been used in clinical trials for new therapeutics. Stroobants et al performed FDG-PET 8 days after the start of therapy to assess the efficacy of imatinib (Gleevac) treatment for gastrointestinal stromal tumors (GIST) and found that 92% of patients with negative FDG-PET scans had 1-year progression-free survival (PFS), whereas only 12% of patients with positive post-treatment FDG-PET scans had 1-year PFS.[50] Currently, treatment monitoring with FDG-PET to assess for tumor response appears to be the most promising functional imaging alternative to structurally based RECIST criteria using CT or MRI alone.

Despite its strengths, FDG-PET has some limitations. FDG-PET is of limited use for slowly growing tumors with minimal glucose metabolism such as bronchioloalveolar cell lung carcinoma, prostate cancer, thyroid cancer, and carcinoid tumor.[40] Due to its limited spatial resolution, PET in general underestimates accurate radiotracer concentration in small lesions, and thus may not always be sensitive enough as a single modality to detect and monitor certain malignancies, although PET/CT may overcome some of these deficiencies. Another limitation of FDG-PET relates to the physiologic biodistribution of FDG in the kidneys and collecting systems, as well as in the bowel, which may obscure uptake in lesions located in adjacent tissues. However, PET/CT with oral contrast can diminish this deficiency by providing coregistered structural and metabolic images, allowing for more accurate localization of sites of FDG uptake.[51] Lastly, FDG uptake may be seen in sites of infection or inflammation, potentially leading to a false-positive diagnosis of sites of malignancy. However, specificity can be improved through dual-time-point imaging, where PET images are obtained at 2 separate time points on the same day of examination. Malignancies often demonstrate an increase in FDG uptake over time, whereas infectious or inflammatory lesions tend to demonstrate no change or a decrease in FDG uptake over time.[52] Specificity can also be improved on through certain CT morphologic features of lesions that may strongly indicate benignity.

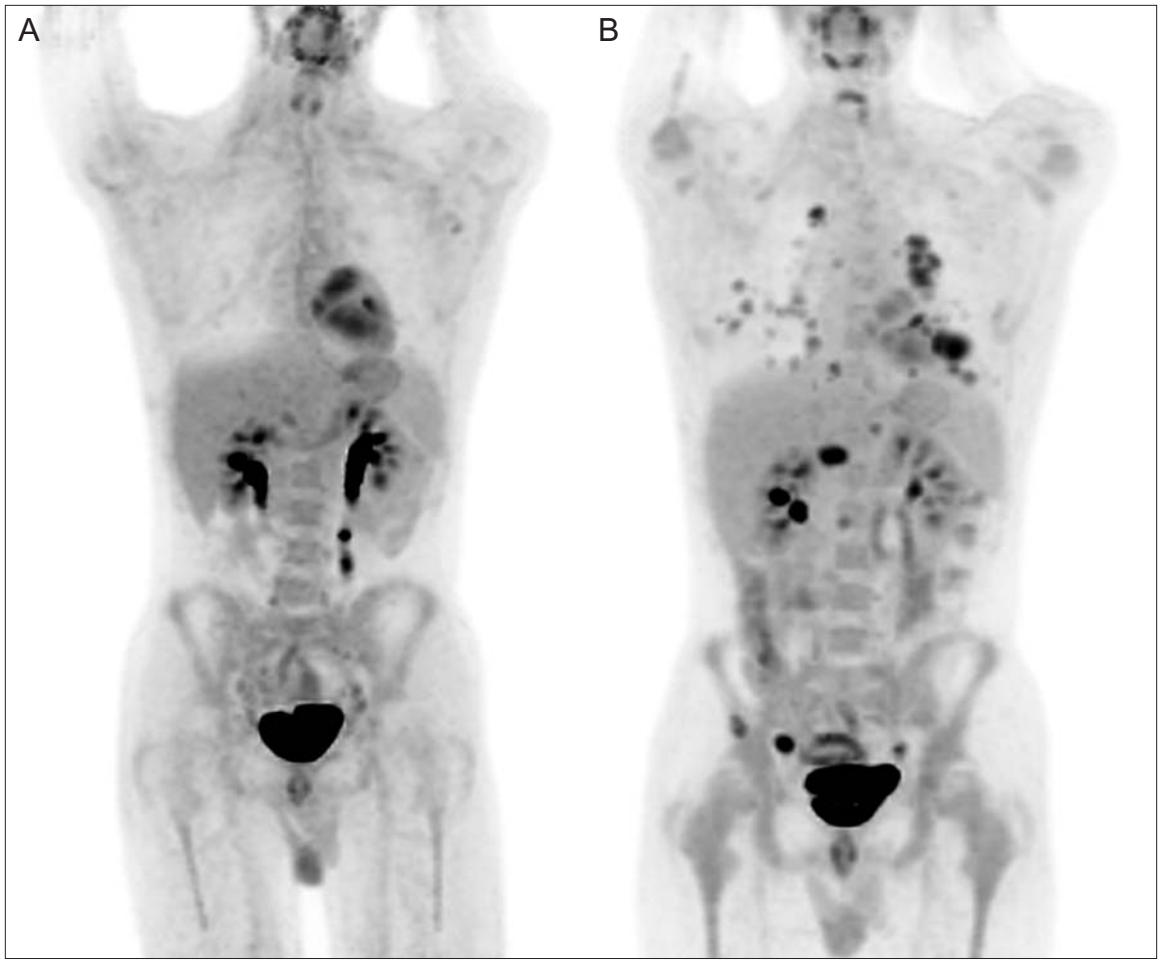

FIGURE **7** FDG-PET Treatment Monitoring of Hodgkin Disease. (A) and (B) Three-dimensional coronal whole-body FDG-PET images at baseline and after 4 cycles of chemotherapy show marked progression of disease in abdomen with new lesions in liver and retroperitoneal lymph nodes. Also noted is confluent parenchymal disease in left lower lobe of lung and multiple pulmonary nodules.

Amino Acid Metabolism

Analogues of methionine, tyrosine, and L-dihydroxyphenylalanine (L-DOPA) have potential for widespread clinical application and sometimes have better diagnostic performance characteristics in certain PET applications when compared with those utilizing FDG. ^{11}C-L-methionine is chemically identical to nonradioactive L-methionine. Consequently, it is metabolized and trapped in the cell by incorporation into proteins or even RNA molecules.[53] Advantages of imaging brain tumors with ^{11}C-methionine are well documented, as there is low background uptake of ^{11}C-methionine in the brain. A recent study by Jacobs et al showed a sensitivity of 91% for detecting gliomas, as well as larger detected tumor volumes compared with those detected with Gd-enhanced MRI, which may have an impact on radiation treatment planning.[54] However, the major shortcoming of ^{11}C-methionine is the 20-minute half-life of the ^{11}C isotope, although ^{18}F-fluorinated amino acid analogues have been developed to overcome this limitation since ^{18}F has a 109-minute half-life.

Tyrosine analogues such as L-3–^{18}F-fluoro-α-methyl tyrosine (FMT) and O-(2–^{18}F-fluoroethyl) L-tyrosine (FET) may be of clinical value in imaging certain tumors. For example, FMT-PET had a sensitivity of 73% and a specificity of 85% in a series of 75 patients with musculoskeletal tumors (whereas the specificity of FDG-PET was lower at 66%).[55]

^{18}F-6-fluorodihydroxyphenylalanine (^{18}F-FDOPA), an analogue of L-DOPA, accumulates in dopaminergic neurons in the basal

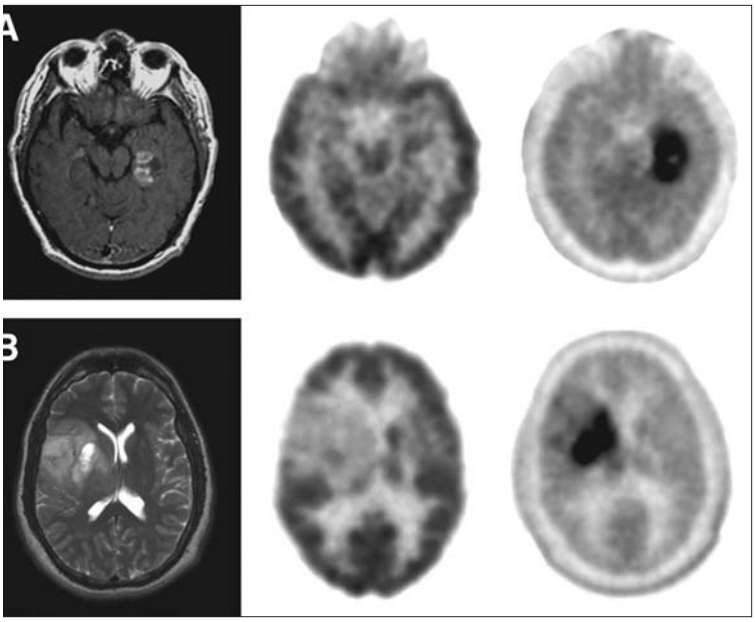

GURE **8** FDG-PET and FLT-PET Assessment of Malignant Brain Tumors. .) and (B) Axial T1-weighted and T2-weighted images, respectively, show 2 het- ogeneous malignant brain tumors. Middle column and right column, axial DG-PET and FLT-PET images, respectively, through brain tumors show high ensitivity of latter for detection of active brain tumor. High uptake of FDG in cor- x and subcortical nuclei results in low contrast between lesions and surround- g structures. FLT allows visualization of rapidly proliferating malignant cells in ain tumors and may allow early detection of response to cytotoxic chemothera- eutic agents. Figures courtesy of Alex Spence, MD, University of Washington.

ganglia and can be used to study patients with melanoma, carcinoid tumor, medullary thyroid cancer, and brain tumors.[56] A recent study with FDOPA-PET in 19 patients with abdominal carcinoid tumors showed 93% sensitivity and 89% accuracy.[57] FDOPA-PET has also been shown to be more accurate than FDG-PET for evaluation of low-grade and recurrent brain tumors and for differentiation of low-grade tumors from necrosis.[58]

Cell Proliferation Imaging

Cell proliferation imaging assesses the uptake and metabolism of nucleosides used in nucleic acid synthesis. The most widely used nucleoside analogue for cell proliferation imaging to date is 3′-deoxy-3′-^{18}F-fluorothymidine (FLT), which enters cells through carrier-mediated diffusion.[59] The tracer is trapped when a thymidine kinase (TK) such as TK1 phosphorylates FLT to fluorothymidine-phosphate, which cannot be metabolized further. Shields et al was the first to propose the use of FLT-PET to measure cellular TK activity and thereby infer the rate of cellular proliferation.[60] Overall, FLT-PET has lower sensitivity compared with FDG-PET and amino acid analogue PET for the detection of cancer. However, FLT-PET provides images for rates of proliferation, whereas most other tracers do not (Figure 8). The specificity of FLT for assessment of cellular-proliferative activity makes it an ideal tracer for monitoring tumor treatment response, especially when antiproliferative cytostatic agents are employed. For example, Yang et al tested radiation treatment monitoring with FLT-PET in mouse tumor models and found decreased FLT uptake 24 hours after radiation treatment with no detectable change in FDG uptake. This suggests that FLT-PET can shorten the timeframe to detect a therapeutic response and may become an effective tool for monitoring treatment.[61]

Oxygenation Imaging

Tumor hypoxia triggers tumor angiogenesis, may be a factor in the activation of extracellular matrix-degrading proteases, and is associated with tumor progression, likelihood of metastatic tumor spread, and poor clinical outcome. However, there may be marked variability of intratumoral, as well as intertumoral, oxygen tension values, and hypoxic tumor cells are generally more radioresistant and possibly more chemoresistant than normoxic tumor cells.[62,63] Thus, ability to identify hypoxic tumor tissue noninvasively may be valuable to identify those patients who may benefit from intensity-modulated radiation therapy (IMRT) or other new treatment strategies such as photodynamic therapy.[62,64]

Nitroimidazole-based compounds such as ^{18}F-fluoromisonidazole (FMISO) are currently the most widely used agents to image hypoxia with PET. Fluoromisonidazole is a lipophilic compound that binds to intracellular proteins in live cells with active mitochondria when oxygen concentration is below 20 mmHg.[65] In a recent study of 58 patients with head and neck cancer, pretherapy FMISO-PET had independent prognostic value.[66] In addition, FMISO-PET can be used to monitor chemoradiation therapy in patients with advanced head and neck cancer where early resolution of FMISO uptake

during treatment is associated with excellent locoregional control.[67]

^{64}Cu(II)-diacetyl-bis(N4-methylthiosemicarbazone) (^{64}Cu-ATSM) is another tracer that is used to image hypoxia.[68] In hypoxic cells, the redox state of the copper atom changes, and ^{64}Cu becomes trapped in mitochondria after dissociation of the Cu-ATSM complex. However, recent animal testing using various tumor models shows that ^{64}Cu-ATSM is a valid PET hypoxia marker in some, but not all, tumor types, implying that it may not be useful as a general hypoxia imaging agent.[69]

^{18}F-EF5, a 2-nitroimidazole analogue, is another potential positron-emitting hypoxia tracer.[70] Hypoxic regions delineated by ^{18}F-EF5-PET have been shown to influence patient survival and lack of response to radiation treatment, and preliminary tests of ^{18}F-EF5 in patients with head and neck and brain tumors show promising results.[71,72]

Blood oxygen level-dependent (BOLD) functional MRI (fMRI) has been used as a noninvasive method to preoperatively map functional cerebral cortex and to identify eloquent areas of the cerebral cortex in relation to brain cancers, potentially reducing the time of surgery and minimizing intraoperative cortical stimulation methods, which are sometimes used during the surgical resection of brain tumors.[73,74] In addition, BOLD fMRI, as well as other functional MRI techniques such as Overhauser-enhanced MRI and electron paramagnetic resonance imaging (EPRI), may be useful to study oxygenation in human tumors and to monitor changes in tumors related to therapy.[75,76]

Molecular Imaging with Targeted Imaging Agents

Somatostatin Receptors

Somatostatin receptors (SSTRs) are overexpressed in many neuroendocrine tumors, including small-cell lung cancer, carcinoid tumor, insulinoma, VIPoma, gastrinoma, and medullary thyroid cancer. Whole-body SSTR imaging is performed with radiolabeled derivatives of octreotide, which have a preference for subtype 2 SSTRs (ie, $SSTR_2$). The most commonly used agent is ^{111}In-pentetreotide for SPECT imaging, although SSTR-targeted tracers have also been developed for PET, including ^{68}Ga-D-Phe1-Tyr3-octrotide (^{68}Ga-DOTATOC) and Gluc-Lys(^{18}F-fluoropropionyl-TOCA). Meisetschlager et al used Gluc-Lys(^{18}F-fluoropropionyl-TOCA)-PET to study 25 patients with SSTR-positive tumors. Compared with ^{111}In-pentetreotide SPECT, Gluc-Lys(^{18}F-fluoropropionyl-TOCA)-PET revealed more than twice the number of lesions and resulted in near-perfect interobserver agreement. Gluc-Lys(^{18}F-fluoropropionyl-TOCA) also demonstrated better biodistribution, biokinetics, and diagnostic performance in comparison with ^{68}Ga-DOTATOC in the assessment of neuroendocrine tumors.[77]

Estrogen Receptors

Currently, in vitro examination of biopsy specimens with immunohistochemistry is required to assess levels of estrogen receptor (ER) expression, although not all tumor sites are accessible by biopsy. ER targeting tracers, therefore, may be used to noninvasively assess the ER status of tumors in vivo through use of ^{18}F fluorinated estrogen analogues, and 16α-^{18}F-fluoroestradiol-17β (FES) is commonly used for this purpose due to its favorable biodistribution.[59] FES-PET may show a faster treatment response than FDG-PET at 7 to 10 days after treatment initiation when monitoring breast cancer therapy using tamoxifen.[78] FES-PET may also assist in the selection of the appropriate therapy for breast cancer patients. Use of FES-PET may increase overall response rate following therapy with tamoxifen from 23% to 34%, and for patients with HER2/neu-negative breast cancer, treatment response may improve from 29% to 46% if selection is made using FES-PET.[79]

Angiogenesis Imaging

Angiogenesis, the formation of new blood vessels, is now the target of many new therapeutic agents.[80,81] Perfusion imaging as described above can indirectly provide information about tumor angiogenesis, although some tumors may have dense but mostly quiescent endothelium that is resistant to antiangiogenic therapy. Accurate assessment of angiogenesis thus requires approaches that can directly quantify activated endothelial cells, such as through detection of

$\alpha_V\beta_3$ integrins that are present on activated endothelial cells undergoing angiogenesis.[82]

Peptides containing the amino acid sequence arginine-glycine-aspartate (RGD) have a general affinity toward integrins. It has been shown that fine-tuning of the stereochemistry adjoining the RGD peptide allows for selective binding to specific integrins.[83,84] This led to the development of RGD-based pentapeptide integrin antagonists, such as EMD 121974 (Cilengitide), which can be used to inhibit tumor angiogenesis.[85,86] ^{18}F-labeled RGD compounds have also been synthesized to allow for rapid visualization of $\alpha_V\beta_3$ expression in the whole body using PET.[87] For example, ^{18}F-galacto-RGD PET was used by Beer et al in 19 patients with various solid tumors. Tumoral uptake of ^{18}F-galacto-RGD correlated with $\alpha_V\beta_3$ expression, as well as microvessel density as observed at histology.[88] Thus, ^{18}F-galacto-RGD PET has potential use for individualized treatment planning and antiangiogenic therapy monitoring, although a drawback is that it binds to $\alpha_V\beta_3$ integrins present on the membranes of tumor cells, as well as membranes of tumor-associated endothelial cells. As such, imaging agents based on targeting of cell receptors, such as vascular endothelial cell growth factor receptor, that are overexpressed on endothelial cells during angiogenesis are currently under development. Nevertheless, ability to quantify total tumor $\alpha_V\beta_3$ integrin levels is important, given that $\alpha_V\beta_3$ expression by tumor cells is linked to increased metastatic potential.[89]

Apoptosis Imaging

Apoptosis, or programmed cell death, is a characteristic feature of normal human cells that is essential for normal tissue homeostasis and tissue differentiation.[90] However, tumor growth is often associated with insufficient apoptosis. In vivo imaging of apoptosis offers another noninvasive approach to monitor therapeutic response independent of changes in glucose metabolism or cell proliferation.[91] Annexin V binds to phosphatidylserine (PS) that has moved to the outer surface of cell membranes during apoptosis and can be labeled with either ^{99m}Tc, ^{124}I, or ^{18}F to image apoptosis in vivo using SPECT or PET, respectively.[92] OI of apoptosis in preclinical animal models or in vitro is also possible using Annexin V labeled with Cy5.5, a near-infrared fluorescent dye.[93] The source of light emission for fluorescent imaging is either from fluorescent organic compounds called fluorophores or semiconductor-based nanoparticles called quantum dots.[38]

Superparamagnetic iron-based contrast agents, as well as other paramagnetic contrast agents in conjunction with targeted carrier nanoparticles, are also under development in animal models to specifically target particular molecules or biologic processes for detection, predominantly using MRI.[94,95] For example, Schmieder et al noninvasively characterized melanoma in its earliest phase of growth in mice using $\alpha_V\beta_3$-targeted paramagnetic nanoparticles to detect $\alpha_V\beta_3$ integrin expression in tumor neovasculature using MRI, and Schellenberger et al have used nanoparticles conjugated to Annexin V to target apoptosis for noninvasive monitoring using MRI or OI.[96,97] However, limitations of such approaches using MRI for detection include low signal-to-noise ratio with low sensitivity, lack of standardization of imaging and analytic methodologies, and inconsistent availability of these new technologies at sites around the country.[1,98]

Magnetic Resonance Spectroscopy

Magnetic resonance spectroscopy (MRS) is a noninvasive diagnostic tool that allows one to quantitatively assess the amount, type, and location of various small molecular compounds within a tissue or organ of interest at the same time that MRI is performed. It does so by taking advantage of the quantum-mechanical properties of the nuclei of certain atomic isotopes, which permit them to be manipulated through the application of magnetic fields and radiofrequency pulses. The data are typically displayed as a grid of spectra of chemical compound abundances obtained at either single or multiple locations in a tissue or organ of interest. These spectra are collected from spinning nuclei (spins), most often ^{1}H given the abundance of water in tissue, although they can be collected from other nuclei such as ^{13}C or ^{31}P with more

difficulty due to lower tissue concentrations.[99] Proton ^{1}H MRS enables accurate quantitative assessment of the spatial distribution of tissue metabolites such as creatinine, choline, amino acids, nucleotides, lactate, and lipids.[100] Unfortunately, there is no one cancer signature on MRS, but there are MRS findings that are seen more often in cancer.[99] For example, increased concentrations of cell membrane metabolites such as phosphocholine may be seen due to increased membrane synthesis, a higher concentration of lactate may be seen due to increased metabolism through the glycolytic pathway, and lower concentrations of normal tissue metabolites (such as N-acetyl aspartate in cerebral tissue or citrate in prostatic tissue) may be encountered (Figure 2).[101,102]

^{1}H MRS is most often applied clinically to evaluate brain tumors due to the relative lack of motion artifact in this location relative to other body sites. As such, many single-center studies of ^{1}H MRS in the setting of brain cancer have been reported.[99] In patients with gliomas, ^{1}H MRS and perfusion-MRI analysis provide complementary information to assess tumor grade and to detect residual or recurrent tumor. ^{1}H MRS enables better discrimination between normal and abnormal tissue than regional cerebral blood-flow maps, whereas regional cerebral blood-flow maps may better reflect the heterogeneity of tumor regions because of their higher resolution.[103] In addition, ^{1}H MRS may be useful to predict patient prognosis. Oh et al reported that patients with glioblastoma multiforme had significantly shorter median survival when a large volume of metabolic abnormality was seen at ^{1}H MRS.[104] Many investigators have also demonstrated significant spatial discordance between morphologic lesions and metabolic lesions using ^{1}H MRS in brain tumors, which has significant implications with regard to treatment planning for surgery and/or radiotherapy.[104,105] Moreover, ^{1}H MRS can be used to distinguish pyogenic brain abscesses from cystic or necrotic brain tumors, gliomas from solitary brain metastases, and residual or recurrent brain tumor from post-therapy radiation necrosis.[106–108]

^{1}H MRS has occasionally been applied to study tumors in other body locations. Swindle et al reported that ^{1}H MRS has a high sensitivity (97%) and specificity (88%) for prostate carcinoma.[109] Furthermore, ^{1}H MRS can lead to more accurate assessment of the presence, location, and extent of prostate cancer; may reveal overall tumor clinicopathologic status and aggressiveness; and can be used to assess therapeutic response.[110] ^{1}H MRS has also been used to study tumors of the breast, pancreas, cervix, and thyroid gland.[111]

^{31}P MRS also has potential utility to noninvasively assess tumors. It has shown some promise to differentiate prostate carcinoma from benign prostatic hypertrophy.[112] Others have shown that it can differentiate benign from malignant head and neck neoplasms and can predict treatment response and monitor therapeutic effects for head and neck cancer.[113] Arias-Mendoza et al reported that ^{31}P MRS pretreatment measurement of phosphoethanolamine and phosphocholine content within non-Hodgkin lymphoma predicts long-term response to treatment and time-to-treatment failure, particularly when combined with the international prognostic index.[114]

Research efforts directed toward use of hyperpolarized ^{13}C MRI/MRS agents for metabolic and molecular imaging are currently underway, although many technical challenges still exist. ^{13}C MRI/MRS has the potential to provide information about any molecule that contains hyperpolarized ^{13}C and to distinguish between different molecules that contain ^{13}C atoms. This suggests the potential utility of this approach to study carbon-based compounds in vivo for oncologic applications such as tumor perfusion and metabolism assessment, as well as new drug pharmacokinetic and pharmacodynamic assessment.[115]

Although MRS has been around for several decades and can sensitively detect and characterize metabolites within tumors and nonneoplastic tissue, it is still considered to be a prebiomarker by most investigators as it is not yet fully established as reproducible across multiple institutions. Difficulties in performing multicenter trials with MRS include differences in hardware and software among different sites due to lack of standardization, as well as effects of patient motion.[99]

OTHER APPLICATIONS OF FUNCTIONAL IMAGING TO STUDY TUMORS

Gene Expression and Cell Tracking

Gene expression imaging has been used to study tumor biology and molecular changes in tumors before and after treatment in vitro and in animal models. It is typically performed through detection of an expressed reporter protein, such as a transporter, enzyme, or receptor that is controlled by the regulatory element of a reporter gene of interest. Some examples of reporter proteins include green fluorescent protein (GFP) analogues, luciferase mutants, and herpes simplex virus thymidine kinase (HSV-tk). Depending on the choice of reporter protein and reporter probe, gene expression may be imaged with OI, SPECT, or PET.[116] In general, this technology is difficult to adapt to routine clinical use because it requires the introduction of marker genes and, therefore, is most relevant to in vitro or animal models.

Several investigators have focused on use of OI to study gene expression. For example, Cao et al used GFP linked to hypoxia-inducible factor (HIF-1) promoter in a tumor cell line that expressed red fluorescent protein (RFP) constitutively and was able to differentiate between normoxic tumor cells and hypoxic tumor cells in a growing tumor environment.[117] At present, use of OI to study gene expression in tumors is limited to use in small animals and for superficial human structures such as the breast due to limited light penetration through tissue. Other investigators have focused on PET to study gene expression in tumors. A prototypical reporter protein for use with PET is HSV-tk, which can be imaged following administration of a positron-emitting nucleoside analogue reporter probe that can be phosphorylated and trapped intracellularly by HSV-tk.[118]

Cell tracking is important to study the behavior of tumor cells in vitro and in animal models and can potentially be used to track cellular therapies for cancer, to track stem cells, and to assess the effectiveness of gene therapy against cancer cells.[119] Cell tracking is possible when cells of interest are engineered to constitutively express a reporter protein that is detectable by either OI or PET.[120] For example, Jenkins et al developed bioluminescent prostate cancer and breast cancer models to observe treatment response to chemotherapy using OI.[121] In addition, investigators have introduced luciferase and GFP into genetically transformed cells during gene therapy to monitor efficiency of transfection using OI or PET.[122] Recently, some investigators have successfully performed in vivo cell tracking using MRI in animal models through use of superparamagnetic iron oxide nanoparticles or paramagnetic contrast agents that are introduced into cells, although efforts to translate this approach into humans are currently under active investigation.[123,124]

Molecular Imaging-based Personalized Treatment Planning

Molecular phenotypes of tumors may affect their susceptibility to chemotherapeutic agents, which may be extremely important to know about for individualized treatment planning. For example, epidermal growth factor receptor (EGFR) mutations are found in about 10% of NSCLC, and patients with these mutations have a statistically significant better outcome following EGFR tyrosine kinase inhibitor therapy with gefitinib (Iressa; AstraZeneca, London, UK).[125] In the remaining 90% of patients without these mutations, unnecessary exposure to this drug may be avoided, leading to monetary savings and fewer adverse events from drug toxicity, as well as earlier use of alternative, more effective therapies.

As seen by this example, the "personalized medicine" paradigm is becoming a reality in treatment planning for many patients with malignancies, particularly as therapeutics are increasingly targeted toward specific cellular receptors. As such, molecular imaging will increasingly become a part of individualized treatment planning and pharmacogenomics. Molecular imaging will increasingly supplement in vitro molecular diagnostic testing of tissue or bodily fluid specimens, as it can be used for quantitative, noninvasive serial evaluation, as well as whole-body assessment of multiple lesions, including those that are in difficult to reach locations. Moreover, molecular imaging using radiolabeled preparations of intended drugs may be used to determine appropriate pharmacological doses on an individualized basis.

An example of this concept is the pretreatment evaluation of pharmacokinetics of radiolabeled antibodies or peptides to be used for therapeutic purposes using PET. In order to predict treatment success using radiolabeled antibodies or peptides against a tumor, it is important to demonstrate appropriate targeting to the diseased tissue. Positron-emitting isotopes such as ^{124}I (as a surrogate for ^{131}I) and ^{86}Y (as a surrogate for ^{90}Y) can be utilized for optimal visualization of these agents to targeted sites and may significantly improve the ability to select optimal patient candidates for subsequent treatment with antibodies or peptides radiolabeled with therapeutic beta-emitting radionuclides. Through this approach, one may identify patients who are good candidates for antibody or peptide treatment by comparing images acquired with nonspecific radiotracers such as FDG that reveal overall disease activity with PET images generated with positron-emitting radiolabeled antibodies or peptides for diagnostic purposes. Since radiolabeled antibodies result in a favorable response if they target the entirety of the tumor burden, disparity between uptake within tumor on the FDG-PET images and diagnostic PET images using radiolabeled antibodies or peptides may indicate a poor outcome following treatment with beta-emitting agents.[126]

New Drug Development

Functional imaging techniques have the potential to accelerate cancer drug development during the preclinical and clinical phases of testing.[127,128] This is especially relevant given the difficulties in both designing targeted cancer therapies and monitoring their efficacy. Tumors may be spatially and temporally heterogeneous in terms of gene expression, metabolism, oxygenation status, angiogenesis, cell proliferation, apoptosis, signal transduction, and other phenotypic features, but functional imaging can help investigators to better understand these features.[127]

As such, functional imaging can aid in molecular target-based drug screening, definition of in vivo target specificity, rapid characterization of in vivo pharmacokinetic and pharmacodynamic properties of candidate drugs, development of animal models of human tumors, and visualization of in vivo effects of therapeutic molecules on target biological processes.[128] These approaches are particularly useful as they could reduce the length of time for developing effective drugs (which usually can take more than a decade) and reduce the costs of drug development (often in the range of hundreds of millions of dollars) during preclinical evaluation and clinical trial assessment.[129,130] For example, any new therapeutics for GIST may use the post-therapy FDG-PET scan as the surrogate endpoint of the trial since the 8-day post-therapy FDG-PET scan has been shown to predict outcome for imatinib treatment.[50] Recently, FLT-PET has been used to monitor the preclinical testing of histone deacetylase inhibitors (HDACI), an expanding class of growth-inhibiting compounds targeting DNA and RNA. In animal models of colon carcinoma, Leyton et al reported that decreasing FLT uptake in tumor correlates with escalating doses of LAQ824, a new HDACI, and that the quantity of FLT uptake correlates with decreased expression of thymidine kinase 1 (TK1).[131]

Transformation of therapeutic compounds themselves into imaging agents and testing for the presence of the compound at intended target sites is another way functional imaging can be used to facilitate drug development. ^{18}F, ^{11}C, and ^{13}N PET can offer this possibility given its high sensitivity. Similarly, ^{19}F and ^{31}P MRS can be used for the detection, identification, and quantification of fluorine-containing or phosphorous-containing therapeutic agents, and their metabolites in biofluids may play a role in the therapeutic monitoring of fluorinated or phosphorylated chemotherapeutic drugs such as fluorouracil and cyclophosphamide, respectively, in specific groups of patients and may provide further understanding into drug metabolic pathways. However, the main challenge to widespread application of these MRS techniques is a more limited sensitivity in the micromolar-millimolar concentration range.[132,133]

CONCLUSION

A wide variety of functional imaging techniques are currently under active investigation that have great potential to noninvasively

provide never before available quantitative information regarding physiologic and biological properties of tumors at the molecular, subcellular, cellular, tissue, organ, and systemic levels unavailable from routine structural imaging techniques alone. Such functional imaging techniques will enhance the efficiency and effectiveness of oncologic research, will help to characterize biomarkers of disease and new endpoints for assessment of tumor response, and will positively impact those with cancer due to improvements in early detection, characterization, staging, and monitoring of therapeutic response of tumors, as well as improvements in individualized treatment planning, prognosis assessment, and cell tracking. Thus, we believe that quantitative functional imaging, in conjunction with quantitative structural imaging, will be the future of "personalized radiology," "personalized oncology," "personalized medicine," and of oncologic research in the 21st century and beyond.

ACKNOWLEDGEMENTS

We would like to thank Sumei Wang, MD, Gul Moonis, MD, and Elias R. Melhem, MD, PhD, from the University of Pennsylvania, and Alex Spence, MD, from the University of Washington for providing figures for this scientific communication.

REFERENCES

1. Atri M. New technologies and directed agents for applications of cancer imaging. J Clin Oncol 2006;24:3299–3308.

2. Alavi A, Lakhani P, Mavi A, et al. PET: a revolution in medical imaging. Radiol Clin North Am 2004;42:983–1001.

3. Pieterman RM, van Putten JW, Meuzelaar JJ, et al. Preoperative staging of non-small-cell lung cancer with positron-emission tomography. N Engl J Med 2000;343:254–261.

4. Therasse P, Arbuck SG, Eisenhauer EA, et al. New guidelines to evaluate the response to treatment in solid tumors. European Organization for Research and Treatment of Cancer, National Cancer Institute of the United States, National Cancer Institute of Canada. J Natl Cancer Inst 2000; 92:205–216.

5. Therasse P, Eisenhauer EA, Verweij J. RECIST revisited: a review of validation studies on tumour assessment. Eur J Cancer 2006;42:1031–1039.

6. Schnall M, Rosen M. Primer on imaging technologies for cancer. J Clin Oncol 2006;24:3225–3233.

7. Aksoy FG, Lev MH. Dynamic contrast-enhanced brain perfusion imaging: technique and clinical applications. Semin Ultrasound CT MR 2000; 21:462–477.

8. Miles KA. Tumour angiogenesis and its relation to contrast enhancement on computed tomography: a review. Eur J Radiol 1999;30:198–205.

9. Padhani AR, Leach MO. Antivascular cancer treatments: functional assessments by dynamic contrast-enhanced magnetic resonance imaging. Abdom Imaging 2005;30:324–341.

10. Hylton N. Dynamic contrast-enhanced magnetic resonance imaging as an imaging biomarker. J Clin Oncol 2006;24:3293–3298.

11. George ML, Dzik-Jurasz AS, Padhani AR, et al. Non-invasive methods of assessing angiogenesis and their value in predicting response to treatment in colorectal cancer. Br J Surg 2001;88: 1628–1636.

12. Erdogan C, Hakyemez B, Yildirim N, Parlak M. Brain abscess and cystic brain tumor: discrimination with dynamic susceptibility contrast perfusion-weighted MRI. J Comput Assist Tomogr 2005;29:663–667.

13. Leach MO, Brindle KM, Evelhoch JL, et al. The assessment of antiangiogenic and antivascular therapies in early-stage clinical trials using magnetic resonance imaging: issues and recommendations. Br J Cancer 2005;92:1599–1610.

14. Miles KA, Charnsangavej C, Lee FT, et al. Application of CT in the investigation of angiogenesis in oncology. Acad Radiol 2000;7:840–850.

15. Miles KA. Functional CT imaging in oncology. Eur Radiol 2003;13(suppl):M134–M138.

16. Tateishi U, Kusumoto M, Nishihara H, et al. Contrast-enhanced dynamic computed tomography for the evaluation of tumor angiogenesis in patients with lung carcinoma. Cancer 2002; 95:835–842.

17. Ng QS, Goh V, Fichte H, et al. Lung cancer perfusion at multi-detector row CT: reproducibility of whole tumor quantitative measurements. Radiology 2006;239:547–553.

18. Gee MS, Saunders HM, Lee JC, et al. Doppler ultrasound imaging detects changes in tumor perfusion during antivascular therapy associated with vascular anatomic alterations. Cancer Res 2001; 61:2974–2982.

19. Robbin ML. Ultrasound contrast agents: a promising future. Radiol Clin North Am 2001; 39:399–414.

20. Su JM, Huang YF, Chen HH, et al. Three-dimensional power doppler ultrasound is useful to monitor the response to treatment in a patient with primary papillary serous carcinoma of the peritoneum. Ultrasound Med Biol 2006;32:623–626.

21. Le Bihan D, Poupon C, Amadon A, Lethimonnier F. Artifacts and pitfalls in diffusion MRI. J Magn Reson Imaging 2006;24:478–488.

22. Chenevert TL, Meyer CR, Moffat BA, et al. Diffusion MRI: a new strategy for assessment of cancer therapeutic efficacy. Mol Imaging 2002; 1:336–343.

23. Mascalchi M, Filippi M, Floris R, et al. Diffusion-weighted MR of the brain: methodology and clinical application. Radiol Med (Torino) 2005;109:155–197.

24. Hamstra DA, Chenevert TL, Moffat BA, et al. Evaluation of the functional diffusion map as an early biomarker of time-to-progression and overall survival in high-grade glioma. Proc Natl Acad Sci USA 2005;102:16759–16764.

25. Hein PA, Eskey CJ, Dunn JF, Hug EB. Diffusion-weighted imaging in the follow-up of treated high-grade gliomas: tumor recurrence versus radiation injury. AJNR Am J Neuroradiol 2004;25:201–209.

26. Bukte Y, Paksoy Y, Genc E, Uca AU. Role of diffusion-weighted MR in differential diagnosis of intracranial cystic lesions. Clin Radiol 2005; 60:375–383.

27. Guo AC, Cummings TJ, Dash RC, Provenzale JM. Lymphomas and high-grade astrocytomas: comparison of water diffusibility and histologic characteristics. Radiology 2002;224:177–183.

28. Le Bihan D, Mangin JF, Poupon C, et al. Diffusion tensor imaging: concepts and applications. J Magn Reson Imaging 2001;13:534–546.

29. Cruz LC Jr, Sorensen AG. Diffusion tensor magnetic resonance imaging of brain tumors. Magn Reson Imaging Clin N Am 2006;14:183–202.

30. Pickles MD, Gibbs P, Lowry M, Turnbull LW. Diffusion changes precede size reduction in neoadjuvant treatment of breast cancer. Magn Reson Imaging 2006;24:843–847.

31. Woodhams R, Matsunaga K, Iwabuchi K, et al. Diffusion-weighted imaging of malignant breast tumors: the usefulness of apparent diffusion coefficient (ADC) value and ADC map for the detection of malignant breast tumors and evaluation of cancer extension. J Comput Assist Tomogr 2005;29:644–649.

32. Bedrosian I, Scheff AM, Mick R, et al. ^{99m}Tc-human serum albumin: an effective radiotracer for identifying sentinel lymph nodes in melanoma. J Nucl Med 1999;40:1143–1148.

33. Kumar R, Zhuang H, Schnall M, et al. FDG PET positive lymph nodes are highly predictive of metastasis in breast cancer. Nucl Med Commun 2006;27:231–236.

34. Harisinghani MG, Barentsz J, Hahn PF, et al. Noninvasive detection of clinically occult lymph-node metastases in prostate cancer. N Engl J Med 2003;348:2491–2499.

35. Harisinghani MG, Dixon WT, Saksena MA, et al. MR lymphangiography: imaging strategies to optimize the imaging of lymph nodes with ferumoxtran-10. Radiographics 2004;24:867–878.

36. Deserno WM, Harisinghani MG, Taupitz M, et al. Urinary bladder cancer: preoperative nodal staging with ferumoxtran-10-enhanced MR imaging. Radiology 2004;233:449–456.

37. Will O, Purkayastha S, Chan C, et al. Diagnostic precision of nanoparticle-enhanced MRI for lymph-node metastases: a meta-analysis. Lancet Oncol 2006;7:52–60.

38. Levin CS. Primer on molecular imaging technology. Eur J Nucl Med Mol Imaging 2005; 32(suppl):S325–S345.

39. Alavi A, Kung JW, Zhuang H. Implications of PET based molecular imaging on the current and future practice of medicine. Semin Nucl Med 2004;34:56–69.

40. Kelloff GJ, Hoffman JM, Johnson B, et al. Progress and promise of FDG-PET imaging for cancer patient management and oncologic drug development. Clin Cancer Res 2005;11:2785–2808.

41. Gould MK, Maclean CC, Kuschner WG, et al. Accuracy of positron emission tomography for diagnosis of pulmonary nodules and mass lesions: a meta-analysis. JAMA 2001;285:914–924.

42. Toloza EM, Harpole L, McCrory DC. Noninvasive staging of non-small cell lung cancer: a review of the current evidence. Chest 2003; 123(suppl):137S-146S

43. Juweid ME, Cheson BD. Positron-emission tomography and assessment of cancer therapy. N Engl J Med 2006;354:496–507.

44. Bradley J, Thorstad WL, Mutic S, et al. Impact of FDG-PET on radiation therapy volume delineation in non-small-cell lung cancer. Int J Radiat Oncol Biol Phys 2004;59:78–86.

45. Ciernik IF, Dizendorf E, Baumert BG, et al. Radiation treatment planning with an integrated positron emission and computer tomography (PET/CT): a feasibility study. Int J Radiat Oncol Biol Phys 2003;57:853–863.

46. van Baardwijk A, Baumert BG, Bosmans G, et al. The current status of FDG-PET in tumour volume definition in radiotherapy treatment planning. Cancer Treat Rev 2006;32:245–260.

47. Ahuja V, Coleman RE, Herndon J, Patz EF Jr. The prognostic significance of fluorodeoxyglucose positron emission tomography imaging for patients with nonsmall cell lung carcinoma. Cancer 1998;83:918–924.

48. Weber WA. Positron emission tomography as an imaging biomarker. J Clin Oncol 2006; 24:3282–3292.

49. Ceresoli GL, Chiti A, Zucali PA, et al. Early response evaluation in malignant pleural mesothelioma by positron emission tomography with [18F]fluorodeoxyglucose. J Clin Oncol 2006; 24:4587–4593.

50. Stroobants S, Goeminne J, Seegers M, et al. 18FDG-Positron emission tomography for the early prediction of response in advanced soft tissue sarcoma treated with imatinib mesylate (Glivec). Eur J Cancer 2003;39:2012–2020.

51. Antoch G, Saoudi N, Kuehl H, et al. Accuracy of whole-body dual-modality fluorine-18-2-fluoro-2-deoxy-D-glucose positron emission tomography and computed tomography (FDG-PET/CT) for tumor staging in solid tumors: comparison with CT and PET. J Clin Oncol 2004;22:4357–4368.

52. Matthies A, Hickeson M, Cuchiara A, Alavi A. Dual time point 18F-FDG PET for the evaluation of pulmonary nodules. J Nucl Med 2002; 43:871–875.

53. Ishiwata K, Kubota K, Murakami M, et al. A comparative study on protein incorporation of L-[methyl-3H]methionine, L-[1-14C]leucine and L-2-[18F]fluorotyrosine in tumor bearing mice. Nucl Med Biol 1993;20:895–899.

54. Jacobs AH, Thomas A, Kracht LW, et al. 18F-fluoro-L-thymidine and 11C-methylmethionine as markers of increased transport and proliferation in brain tumors. J Nucl Med 2005;46:1948–1958.

55. Watanabe H, Inoue T, Shinozaki T, et al. PET imaging of musculoskeletal tumours with fluorine-18 alpha-methyltyrosine: comparison with fluorine-18 fluorodeoxyglucose PET. Eur J Nucl Med 2000;27:1509–1517.

56. Hoegerle S, Altehoefer C, Ghanem N, et al. Whole-body 18F dopa PET for detection of gastrointestinal carcinoid tumors. Radiology 2001; 220:373–380.

57. Montravers F, Grahek D, Kerrou K, et al. Can fluorodihydroxyphenylalanine PET replace somatostatin receptor scintigraphy in patients with digestive endocrine tumors? J Nucl Med 2006;47:1455–1462.

58. Chen W, Silverman DH, Delaloye S, et al. 18F-FDOPA PET imaging of brain tumors: comparison study with 18F-FDG PET and evaluation of diagnostic accuracy. J Nucl Med 2006; 47:904–911.

59. Couturier O, Luxen A, Chatal JF, et al. Fluorinated tracers for imaging cancer with positron emission tomography. Eur J Nucl Med Mol Imaging 2004;31:1182–1206.

60. Shields AF, Grierson JR, Dohmen BM, et al. Imaging proliferation in vivo with [F-18]FLT and positron emission tomography. Nat Med 1998;4:1334–1336.

61. Yang YJ, Ryu JS, Kim SY, et al. Use of 3′-deoxy-3′-[18F]fluorothymidine PET to monitor early responses to radiation therapy in murine SCCVII tumors. Eur J Nucl Med Mol Imaging 2006;33:412–419.

62. Vaupel P, Mayer A, Briest S, Hockel M. Hypoxia in breast cancer: role of blood flow, oxygen diffusion distances, and anemia in the development of oxygen depletion. Adv Exp Med Biol 2005;566:333–342.

63. Kirkpatrick JP, Cardenas-Navia LI, Dewhirst MW. Predicting the effect of temporal variations in PO2 on tumor radiosensitivity. Int J Radiat Oncol Biol Phys 2004;59:822–833.

64. Chao KS, Bosch WR, Mutic S, et al. A novel approach to overcome hypoxic tumor resistance: Cu-ATSM-guided intensity-modulated radiation therapy. Int J Radiat Oncol Biol Phys 2001; 49:1171–1182.

65. Rajendran JG, Krohn KA. Imaging hypoxia and angiogenesis in tumors. Radiol Clin North Am 2005;43:169–187.

66. Rajendran JG, Schwartz DL, O'Sullivan J, et al. Tumor hypoxia imaging with [F-18] fluoromisonidazole positron emission tomography in head and neck cancer. Clin Cancer Res 2006; 12:5435–5441.

67. Hicks RJ, Rischin D, Fisher R, et al. Utility of FMISO PET in advanced head and neck cancer treated with chemoradiation incorporating a hypoxia-targeting chemotherapy agent. Eur J Nucl Med Mol Imaging 2005;32:1384–1391.

68. Fujibayashi Y, Taniuchi H, Yonekura Y, et al. Copper-62-ATSM: a new hypoxia imaging agent with high membrane permeability and low redox potential. J Nucl Med 1997;38:1155–1160.

69. Yuan H, Schroeder T, Bowsher JE, et al. Intertumoral differences in hypoxia selectivity of the PET imaging agent 64Cu(II)-diacetyl-bis(N4-methylthiosemicarbazone). J Nucl Med 2006; 47:989–998.

70. Ziemer LS, Evans SM, Kachur AV, et al. Noninvasive imaging of tumor hypoxia in rats using the 2-nitroimidazole 18F-EF5. Eur J Nucl Med Mol Imaging 2003;30:259–266.

71. Evans SM, Hahn S, Pook DR, et al. Detection of hypoxia in human squamous cell carcinoma by EF5 binding. Cancer Res 2000;60:2018–2024.

72. Evans SM, Judy KD, Dunphy I, et al. Comparative measurements of hypoxia in human brain tumors using needle electrodes and EF5 binding. Cancer Res 2004;64:1886–1892.

73. Vlieger EJ, Majoie CB, Leenstra S, Den Heeten GJ. Functional magnetic resonance imaging for neurosurgical planning in neurooncology. Eur Radiol 2004;14:1143–1153.

74. Ogawa S, Lee TM, Kay AR, Tank DW. Brain magnetic resonance imaging with contrast dependent on blood oxygenation. Proc Natl Acad Sci USA 1990;87:9868–9872.

75. Padhani AR. Where are we with imaging oxygenation in human tumours? Cancer Imaging 2005;5:128–130.

76. Krishna MC, Subramanian S, Kuppusamy P, Mitchell JB. Magnetic resonance imaging for in vivo assessment of tissue oxygen concentration. Semin Radiat Oncol 2001;11:58–69.

77. Meisetschlager G, Poethko T, Stahl A, et al. Gluc-Lys([18F]FP)-TOCA PET in patients with SSTR-positive tumors: biodistribution and diagnostic evaluation compared with [111In]DTPA-octreotide. J Nucl Med 2006;47:566–573.

78. Dehdashti F, Flanagan FL, Mortimer JE, et al. Positron emission tomographic assessment of "metabolic flare" to predict response of metastatic breast cancer to antiestrogen therapy. Eur J Nucl Med 1999;26:51–56.

79. Linden HM, Stekhova SA, Link JM, et al. Quantitative fluoroestradiol positron emission tomography imaging predicts response to endocrine treatment in breast cancer. J Clin Oncol 2006; 24:2793–2799.

80. Folkman J, Merler E, Abernathy C, Williams G. Isolation of a tumor factor responsible for angiogenesis. J Exp Med 1971;133:275–288.

81. Folkman J. Tumor angiogenesis: therapeutic implications. N Engl J Med 1971;285:1182–1186.

82. Haubner R, Wester HJ, Burkhart F, et al. Glycosylated RGD-containing peptides: tracer for tumor targeting and angiogenesis imaging with improved biokinetics. J Nucl Med 2001;42:326–336.

83. Belvisi L, Bernardi A, Colombo M, et al. Targeting integrins: insights into structure and activity of cyclic RGD pentapeptide mimics containing azabicycloalkane amino acids. Bioorg Med Chem 2006;14:169–180.

84. Pierschbacher MD, Ruoslahti E. Influence of stereochemistry of the sequence Arg-Gly-Asp-Xaa on binding specificity in cell adhesion. J Biol Chem 1987;262:17294–17298.

85. Friess H, Langrehr JM, Oettle H, et al. A randomized multi-center phase II trial of the angiogenesis inhibitor Cilengitide (EMD 121974) and gemcitabine compared with gemcitabine alone in advanced unresectable pancreatic cancer. BMC Cancer 2006;6:285.

86. Albert JM, Cao C, Geng L, et al. Integrin alpha v beta 3 antagonist Cilengitide enhances efficacy of radiotherapy in endothelial cell and non-small-cell lung cancer models. Int J Radiat Oncol Biol Phys 2006;65:1536–1543.

87. Liu S. Radiolabeled multimeric cyclic RGD peptides as integrin alphavbeta3 targeted radiotracers for tumor imaging. Mol Pharm 2006; 3:472–487.

88. Beer AJ, Haubner R, Sarbia M, et al. Positron emission tomography using [18F]Galacto-RGD identifies the level of integrin alpha(v)beta3 expression in man. Clin Cancer Res 2006;12:3942–3949.

89. Nip J, Shibata H, Loskutoff DJ, et al. Human melanoma cells derived from lymphatic metastases use integrin alpha v beta 3 to adhere to lymph node vitronectin. J Clin Invest 1992;90:1406–1413.

90. Fadeel B, Orrenius S. Apoptosis: a basic biological phenomenon with wide-ranging implications in human disease. J Intern Med 2005; 258:479–517.

91. Blankenberg FG, Tait JF, Strauss HW. Apoptotic cell death: its implications for imaging in the next millennium. Eur J Nuclear Med 2000;27:359–367.

92. Blankenberg FG, Katsikis PD, Tait JF, et al. In vivo detection and imaging of phosphatidylserine expression during programmed cell death. Proc Natl Acad Sci USA 1998;95:6349–6354.

93. Ntziachristos V, Schellenberger EA, Ripoll J, et al. Visualization of antitumor treatment by means of fluorescence molecular tomography with an annexin V-Cy5.5 conjugate. Proc Natl Acad Sci USA 2004;101:12294–12299.

94. Serganova I, Blasberg R. Reporter gene imaging: potential impact on therapy. Nucl Med Biol 2005;32:763–780.

95. Caruthers SD, Winter PM, Wickline SA, Lanza GM. Targeted magnetic resonance imaging contrast agents. Methods Mol Med 2006;124:387–400.

96. Schmieder AH, Winter PM, Caruthers SD, et al. Molecular MR imaging of melanoma angiogenesis with alphanubeta3-targeted paramagnetic nanoparticles. Magn Reson Med 2005;53:621–627.

97. Schellenberger EA, Hogemann D, Josephson L, Weissleder R. Annexin V-CLIO: a nanoparticle for detecting apoptosis by MRI. Acad Radiol 2002;9(suppl):S310–S311.

98. Brindle KM. Molecular imaging using magnetic resonance: new tools for the development of tumour therapy. Br J Radiol 2003;76:S111–S117.

99. Sorensen AG. Magnetic resonance as a cancer imaging biomarker. J Clin Oncol 2006;24:3274–3281.

100. Mountford C, Lean C, Malycha P, Russell P. Proton spectroscopy provides accurate pathology on biopsy and in vivo. J Magn Reson Imaging 2006;24:459–477.

101. Sharma U, Mehta A, Seenu V, Jagannathan NR. Biochemical characterization of metastatic lymph nodes of breast cancer patients by in vitro 1H magnetic resonance spectroscopy: a pilot study. Magn Reson Imaging 2004;22:697–706.

102. Kurhanewicz J, Vigneron DB, Nelson SJ. Three-dimensional magnetic resonance spectroscopic imaging of brain and prostate cancer. Neoplasia 2000;2:166–189.

103. Henry RG, Vigneron DB, Fischbein NJ, et al. Comparison of relative cerebral blood volume and proton spectroscopy in patients with treated gliomas. AJNR Am J Neuroradiol 2000;21:357–366.

104. Oh J, Henry RG, Pirzkall A, et al. Survival analysis in patients with glioblastoma multiforme: predictive value of choline-to-N-acetylaspartate index, apparent diffusion coefficient, and relative cerebral blood volume. J Magn Reson Imaging 2004;19:546–554.

105. Pirzkall A, McKnight TR, Graves EE, et al. MR-spectroscopy guided target delineation for high-grade gliomas. Int J Radiat Oncol Biol Phys 2001;50:915–928.

106. Lai PH, Hsu SS, Lo YK, Ding SW. Role of diffusion-weighted imaging and proton MR spectroscopy in distinguishing between pyogenic brain abscess and necrotic brain tumor. Acta Neurol Taiwan 2004;13:107–113.

107. Fan G, Sun B, Wu Z, et al. In vivo single-voxel proton MR spectroscopy in the differentiation of high-grade gliomas and solitary metastases. Clin Radiol 2004;59:77–85.

108. Rock JP, Hearshen D, Scarpace L, et al. Correlations between magnetic resonance spectroscopy and image-guided histopathology, with special attention to radiation necrosis. Neurosurgery 2002;51:912–919.

109. Swindle P, McCredie S, Russell P, et al. Pathologic characterization of human prostate tissue with proton MR spectroscopy. Radiology 2003;228:144–151.

110. Cheng LL, Burns MA, Taylor JL, et al. Metabolic characterization of human prostate cancer with tissue magnetic resonance spectroscopy. Cancer Res 2005;65:3030–3034.

111. Cho SG, Lee DH, Lee KY, et al. Differentiation of chronic focal pancreatitis from pancreatic carcinoma by in vivo proton magnetic resonance spectroscopy. J Comput Assist Tomogr 2005; 29:163–169.

112. Narayan P, Jajodia P, Kurhanewicz J, et al. Characterization of prostate cancer, benign prostatic hyperplasia and normal prostates using transrectal 31phosphorus magnetic resonance spectroscopy: a preliminary report. J Urol 1991; 146:66–74.

113. Shukla-Dave A, Poptani H, Loevner LA, et al. Prediction of treatment response of head and neck cancers with P-31 MR spectroscopy from pretreatment relative phosphomonoester levels. Acad Radiol 2002;9:688–694.

114. Arias-Mendoza F, Smith MR, Brown TR. Predicting treatment response in non-Hodgkin's lymphoma from the pretreatment tumor content of phosphoethanolamine plus phosphocholine. Acad Radiol 2004;11:368–376.

115. Golman K, Petersson JS. Metabolic imaging and other applications of hyperpolarized 13C1. Acad Radiol 2006;13:932–942.

116. Yu Y, Annala AJ, Barrio JR, et al. Quantification of target gene expression by imaging reporter gene expression in living animals. Nat Med 2000;6:933–937.

117. Cao Y, Li CY, Moeller BJ, et al. Observation of incipient tumor angiogenesis that is independent of hypoxia and hypoxia inducible factor-1 activation. Cancer Res 2005;65:5498–5505.

118. Tjuvajev JG, Avril N, Oku T, et al. Imaging herpes virus thymidine kinase gene transfer and expression by positron emission tomography. Cancer Res 1998;58:4333–4341.

119. Thompson M, Wall DM, Hicks RJ, Prince HM. In vivo tracking for cell therapies. Q J Nucl Med Mol Imaging 2005;49:339–348.

120. Choy G, Choyke P, Libutti SK. Current advances in molecular imaging: noninvasive in vivo bioluminescent and fluorescent optical imaging in cancer research. Mol Imaging 2003;2:303–312.

121. Jenkins DE, Yu SF, Hornig YS, et al. In vivo monitoring of tumor relapse and metastasis using bioluminescent PC-3M-luc-C6 cells in murine models of human prostate cancer. Clin Exp Metastasis 2003;20:745–756.

122. Shah K, Jacobs A, Breakefield XO, Weissleder R. Molecular imaging of gene therapy for cancer. Gene Ther 2004;11:1175–1187.

123. Rogers WJ, Meyer CH, Kramer CM. Technology insight: in vivo cell tracking by use of MRI. Nat Clin Pract Cardiovasc Med 2006; 3:554–562.

124. Arbab AS, Liu W, Frank JA. Cellular magnetic resonance imaging: current status and future prospects. Expert Rev Med Devices 2006;3:427–439.

125. Cappuzzo F, Hirsch FR, Rossi E, et al. Epidermal growth factor receptor gene and protein and gefitinib sensitivity in non-small-cell lung cancer. J Natl Cancer Inst 2005;97:643–655.

126. Dadparvar S, Xiu Y, Srikanthan S, et al. Comparison between FDG-PET and diagnostic radiolabeled anti-CD20 antibody uptake sites. Paper presented at: 51st Annual Meeting of the Society of Nuclear Medicine; June 19–23, 2004; Philadelphia, PA. J Nucl Med 2004;45(suppl):319P.

127. Czernin J, Weber WA, Herschman HR. Molecular imaging in the development of cancer therapeutics. Annu Rev Med 2006;57:99–118.

128. El-Deiry WS, Sigman CC, Kelloff GJ. Imaging and oncologic drug development. J Clin Oncol 2006;24:3261–3273.

129. DiMasi JA, Hansen RW, Grabowski HG. The price of innovation: new estimates of drug development costs. J Health Econ 2003;22:151–185.

130. DiMasi JA. The value of improving the productivity of the drug development process: faster times and better decisions. Pharmacoeconomics 2002;20(suppl):1–10.

131. Leyton J, Alao JP, Da Costa M, et al. In vivo biological activity of the histone deacetylase inhibitor LAQ824 is detectable with 3′-deoxy-3′-[18F]fluorothymidine positron emission tomography. Cancer Res 2006;66:7621–7629.

132. Malet-Martino M, Gilard V, Desmoulin F, Martino R. Fluorine nuclear magnetic resonance spectroscopy of human biofluids in the field of metabolic studies of anticancer and antifungal fluoropyrimidine drugs. Clin Chim Acta 2006; 366:61–73.

133. van Laarhoven HW, Punt CJ, Kamm YJ, Heerschap A. Monitoring fluoropyrimidine metabolism in solid tumors with in vivo (19)F magnetic resonance spectroscopy. Crit Rev Oncol Hematol 2005;56:321–343.

Erratum

In the July/August 2007 issue, the page numbers following the abstracts of 4 articles are missing. They should read as follows:

Cancer Incidence, Mortality, and Associated Risk Factors Among Asian Americans of Chinese, Filipino, Vietnamese, Korean, and Japanese Ethnicities (*CA Cancer J Clin 2007;57:190–205)*

Functional Imaging of Cancer with Emphasis on Molecular Techniques (*CA Cancer J Clin 2007;57:206–224)*

The Lethal Phenotype of Cancer: The Molecular Basis of Death Due to Malignancy (*CA Cancer J Clin 2007;57:225–241)*

Young Adult Oncology: The Patients and Their Survival Challenges (*CA Cancer J Clin 2007;57:242–255)*

The publisher regrets this error and apologizes for any confusion it may have caused.